Available online at www.sciencedirect.com
ScienceDirect
Scripta Materialia 60 (2009) 1097–1100
Scripta MATERIALIA
www.elsevier.com/locate/scriptamat

Texture development in the stir zone of near-α titanium friction stir welds

K.E. Knipling* and R.W. Fonda

Naval Research Laboratory, Code 6356, 4555 Overlook Avenue, SW, Washington, DC 20375, USA

Received 4 December 2008; revised 9 February 2009; accepted 10 February 2009
Available online 28 February 2009

Shear textures in the stir zone of a near-α-titanium friction stir weld were examined by electron backscatter diffraction. The texture matches that of a $D_2(\bar{1}\,\bar{1}\,2)[1\,1\,1]$ bcc simple shear texture that was transformed to hcp according to the Burgers orientation relationship, which aligns $\{1\,1\,0\}_{bcc}$ with $\{0\,0\,0\,1\}_{hcp}$, although there is also evidence of a P_1 hcp shear texture component. Deformation therefore occurred predominantly above the β transus, and the α texture was inherited from a simple shear texture of the β phase. Published by Elsevier Ltd. on behalf of Acta Materialia Inc.

Keywords: Friction stir welding; Titanium alloys; Texture; Electron backscattering diffraction (EBSD)

Friction stir welding (FSW) is a solid-state joining technique invented by The Welding Institute (TWI), Cambridge, UK, in 1991 [1]. In typical FSW, a rotating cylindrical tool, consisting of a pin with a concentric larger diameter shoulder, is plunged into the joint line between two abutting plates. As the rotating tool interacts with the material, a combination of frictional and adiabatic heating softens the material, facilitating material flow about the rotating pin. As the tool is traversed along the joint line, material is continually transferred around the tool and then deposited in its wake, forming a solid-state bond between the two pieces. Since no melting is involved, many problems normally associated with conventional welding are eliminated or reduced (*e.g.*, porosity, solidification cracking, shrinkage, and distortion).

Several studies have investigated the evolution of grain structure and crystallographic texture occurring in FSW, focusing primarily on aluminum [2–12], with comparatively little work on steel [13,14] or titanium [15–17] alloys. The present study investigates the texture developed in the stir zone during FSW of Ti-5111 (Ti-5Al-1Sn-1Zr-1V-0.8Mo, wt.%), a near-α-titanium alloy developed for marine applications requiring superior toughness and corrosion resistance [18].

The weld examined in this study is a bead-on-plate (no seam) weld that was prepared at the Edison Welding Institute with a tungsten-based alloy tool. The 12.7 mm (0.5 in.) thick Ti-5111 plate was prepared by Timet. The FSW tool had a simple geometry with a narrow shoulder and a truncated conical shape without threads, flats, or other features (see Fig. 2 for a schematic of the tool). Welding was performed at 140 rpm and 51 mm min^{-1} (2 in. min^{-1}), corresponding to a 360 μm tool advance per revolution.

Upon completion of the weld, the tool was extracted from the plate which was quenched immediately with cold water to preserve the microstructure generated during welding. A plan-view cross-section through the plate mid-thickness of the deposited weld was prepared for examination by electron backscatter diffraction (EBSD). Metallographic preparation of the specimens was carried out using conventional techniques. Final polishing of the surface was accomplished with a solution of 20% hydrogen peroxide (30%) and 80% colloidal silica solution, followed by etching with Krolls reagent. EBSD experiments were conducted in an FEI Nova 600 NanoLab dual column field-emission gun scanning electron microscope and focused ion beam operating at 18 kV and equipped with the Channel 5 system (HKL Technology, Hobro, Denmark).

Figure 1 shows a transverse cross-section of the deposited weld and a plan-view cross-section of the weld exit hole from the friction stir weld investigated. There is a distinct and abrupt change between the parent baseplate material, consisting of very coarse prior-β grains, and the weld nugget, comprised of small, equiaxed grains containing α laths. The other regions typically ob-

* Corresponding author. Tel.: +1 202 767 2947; fax: +1 202 767 2623; e-mail: knipling@anvil.nrl.navy.mil

1359-6462/$ - see front matter Published by Elsevier Ltd. on behalf of Acta Materialia Inc.
doi:10.1016/j.scriptamat.2009.02.050

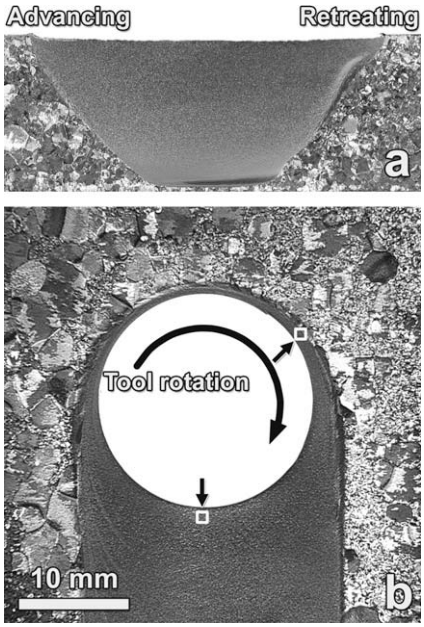

Figure 1. Transverse (a) and mid-thickness plan-view (b) cross-sections of the Ti-5111 friction stir weld. Approximate locations of the regions analyzed by EBSD are indicated by the arrowed regions in (b).

served between the base plate and weld nugget (*i.e.*, the heat affected zone (HAZ) and thermo-mechanically affected zone (TMAZ)) are not apparent in this friction stir weld.

The microstructure observed in the deposited weld consists of small, equiaxed prior-β grains containing laths of α, which indicates that the material around the tool deforms while it is in the high-temperature β phase. Material in the deposited weld transforms back to α after passage of the welding tool, however, preventing a direct observation of the microstructure and texture that existed around the tool during deformation. Nevertheless, the β shear deformation texture can be inferred from the observed α textures within the stir zone. The α deformation texture is related to the high-temperature β deformation texture through the Burgers orientation relationship (OR), which aligns the close-packed planes $\{0001\}_\alpha \| \{110\}_\beta$ and close-packed directions $\langle 11\bar{2}0\rangle_\alpha \| \langle 111\rangle_\beta$ [19]. This Burgers OR is the most commonly observed OR between the α and β phases in titanium [20].

The texture of this Ti-5111 friction stir weld was determined at a number of locations around the tool. Two specific locations — on the retreating side of the weld and in the deposited weld nugget — are shown in Figure 2 and typify the results obtained from the other regions examined. The left-hand pole figures, Figure 2(a), are oriented in the specimen frame of reference (*i.e.*, in plan-view with the welding direction upward). There is a strong texture in both sets of pole figures. The $\langle 11\bar{2}0\rangle_\alpha$ directions are aligned with the tool tangent orientation at each location, which is parallel to the presumed direction of maximum shear. Furthermore, the basal $\{0001\}_\alpha$ planes are consistently perpendicular to the shear direction and tilted $\sim 35^\circ$ from ND in the direction away from the welding tool.

The geometry of the tool can be used to rotate the observed pole figures so that they are oriented in the shear deformation frame of reference, with a horizontal shear direction (SD) and a vertical shear plane normal (SPN). Rotating the pole figure to align the tool tangent along the SD aligns the predominant $\langle 11\bar{2}0\rangle_\alpha$ direction with the horizontal axis of the pole figure. Subsequent rotations about this horizontal SD axis to account for the taper angle of the truncated conical tool nearly aligns a $\langle 10\bar{1}0\rangle_\alpha$ orientation with the SPN and similarly aligns the predominant $\{0001\}_\alpha$ orientation with the radial direction, which lies along the vertical edge of the tapered tool. Thus, the apparent shear frame of reference

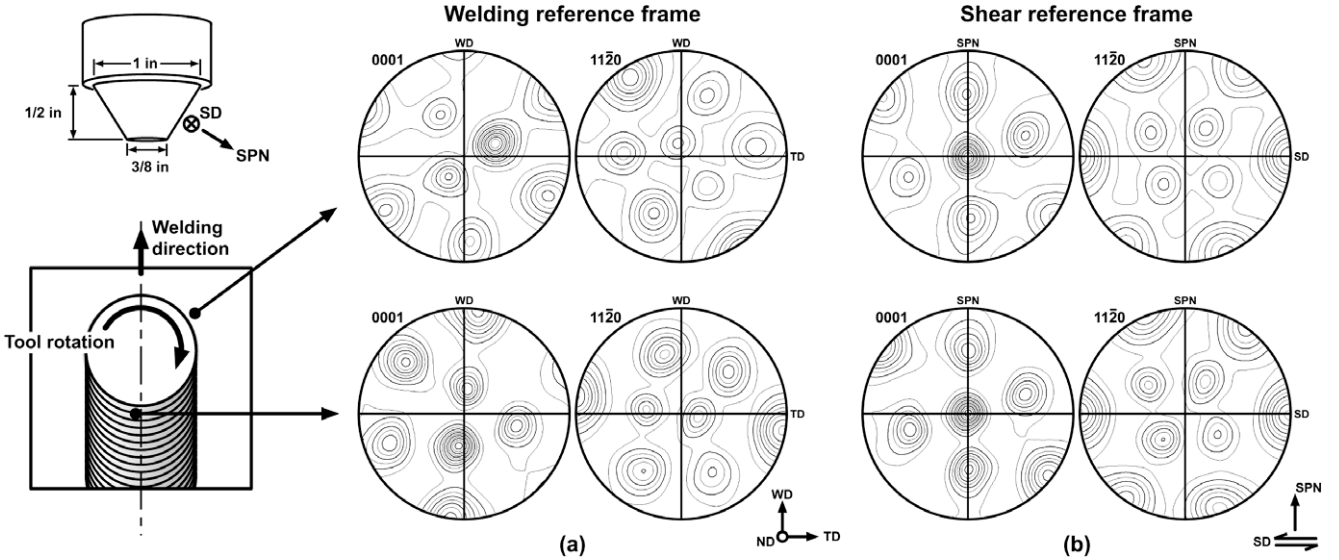

Figure 2. Schematics of the FSW tool geometry and the end of the weld, indicating the locations adjacent to the exit hole from which the $\{0001\}$ and $\{11\bar{2}0\}$ pole figures in parts (a) and (b) (in stereographic projection) were obtained. In (a), the pole figures have the same orientation as the weld schematic. In (b), the pole figures have been rotated to align the presumed shear plane normal (SPN) with the vertical direction and the shear direction (SD) with the horizontal direction. The contours shown in the pole figures are multiples of 0.5 times random density.

aligns the close-packed $\langle 11\bar{2}0\rangle_\alpha$ directions along SD, the $\langle 10\bar{1}0\rangle_\alpha$ directions along the SPN, and the close-packed $\{0001\}_\alpha$ basal planes along the radial direction, perpendicular to both the SD and SPN. The pole figures in Figure 2(b) reflect this local orientation of the texture. The rotations (ϕ_1, Φ, ϕ_2) required to bring the pole figures into this frame of reference are $(-13°, 36°, 68°)$ and $(-2°, -35°, 10°)$ for the regions ahead of the tool and behind the tool, respectively. These rotations reflect the consistent 35° tilt imposed by the tapered tool. The resultant texture is directly comparable to the $B/\bar{B}$ fcc texture reported in aluminum friction stir welds [3,6,10–12], in which the close-packed $\langle 110\rangle_{fcc}$ directions are aligned along SD and the close-packed $\{111\}_{fcc}$ planes are aligned along the radial direction, perpendicular to both the SD and SPN.

The predominant deformation during FSW, particularly in regions close to the tool, is expected to be simple shear, as confirmed in previous FSW studies of aluminum alloys [3,4,6,10–12,21]. In bcc metals, simple shear deformation produces partial fibers belonging to $\{hkl\}\langle 111\rangle$ and $\{110\}\langle uvw\rangle$ types, as revealed by experimental and modeling studies of torsion deformation textures [22–24]. The texture components of these simple shear textures are shown in the $\{110\}_{bcc}$ pole figure, Figure 3(a). Superimposing these $\{110\}_{bcc}$ shear orientations on the $\{0001\}_{hcp}$ pole figure from the deposited weld (shown at the bottom of Fig. 2(b)) shows an excellent agreement between the observed texture and the $D_2(\bar{1}\bar{1}2)[111]$ bcc texture components, as shown in Figure 3(b). This excellent agreement between the experimental $\{0001\}_{hcp}$ texture and the predicted $\{110\}_{bcc}$ shear texture is not unexpected since the Burgers OR aligns these close-packed planes in a parallel orientation. The observed hcp α texture thus appears to be inherited directly from the $D_2(\bar{1}\bar{1}2)[111]$ shear texture of the high-temperature bcc β phase.

In one of the first studies of texture in titanium friction stir welds, Reynolds et al. [16] studied friction stir welds of a β-titanium alloy and observed excellent agreement between the observed shear texture in the weld nugget and the shear textures reported by Rollett and Wright [25] for bcc tantalum. However, Reynolds et al. used a rather significant rotation (30°) about ND to bring their observed shear textures into alignment with the bcc tantalum shear texture. The texture of the present Ti-5111 friction stir weld requires a similar ($\sim 35°$) rotation to align the hcp α texture of this weld with the bcc tantalum shear texture, suggesting that the same $D_2(\bar{1}\bar{1}2)[111]$ texture was produced in both friction stir welds. Indeed, superposition of the textures observed by Reynolds et al. [16] (without the 30° rotation about ND to align with the Rollett and Wright data) onto the present Ti-5111 texture, Figure 4, demonstrates that the β-titanium texture nearly matches (within $\sim 10°$) both the current data and the calculated $D_2(\bar{1}\bar{1}2)[111]$ shear texture. (The $\{11\bar{2}0\}_{hcp}$ texture components without a corresponding $\{111\}_{bcc}$ component in Fig. 4 are the result of an increased multiplicity of the hcp orientations.) These results suggest that there may be a misorientation between the Rollett and Wright bcc tantalum texture and the actual shear frame of reference while confirming that the texture observed after friction stir welding of β-titanium is the same $D_2(\bar{1}\bar{1}2)[111]$ shear texture observed in the present Ti-5111 friction stir weld.

A recent study by Mironov et al. [26] examined the texture that develops in friction stir welds of an α + β-titanium alloy, Ti-6Al-4V. This study concluded that the retained β phase exhibited a $\overline{J}(\bar{1}\bar{1}0)[\bar{1}1\bar{2}]$ shear texture, presumably developed from $\{110\}\langle 111\rangle$ slip. It is not clear why the texture produced in these friction stir welds differs from the $D_2(\bar{1}\bar{1}2)[111]$ shear texture observed in both the β-titanium and Ti-5111 welds, although Mironov et al. recognized that their conclusions were based on a "very limited number of orientation measurements" from the retained β phase.

Mironov et al. [27] also examined the texture that develops during friction stir processing of pure iron. In that study, they consistently observed a $D_2(\bar{1}\bar{1}2)[111]$ simple shear texture from several locations within the stir zone, similar to the shear textures observed in both the β-titanium and the present Ti-5111 friction stir welds. This $D_2(\bar{1}\bar{1}2)[111]$ shear texture is also the most commonly observed texture component that results from equal channel angular extrusion of bcc iron [28,29].

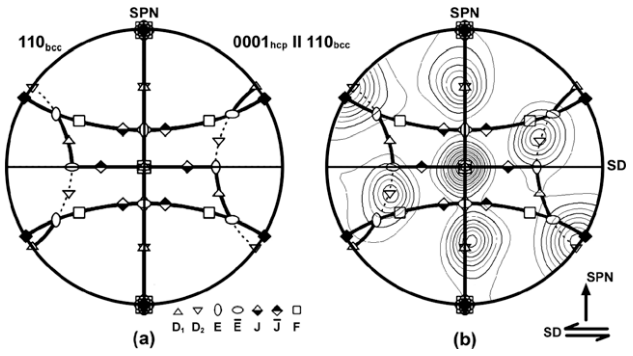

Figure 3. (a) Schematic $\{110\}_{bcc}$ pole figure (in stereographic projection) showing the main texture component orientations and fibers associated with simple shear deformation of bcc metals (after Li et al. [28]). (b) Superposition of the $\{110\}_{bcc}$ simple shear texture components on the $\{0001\}_{hcp}$ pole figure of the deposited weld (rotated into the shear reference frame) from Figure 2(b).

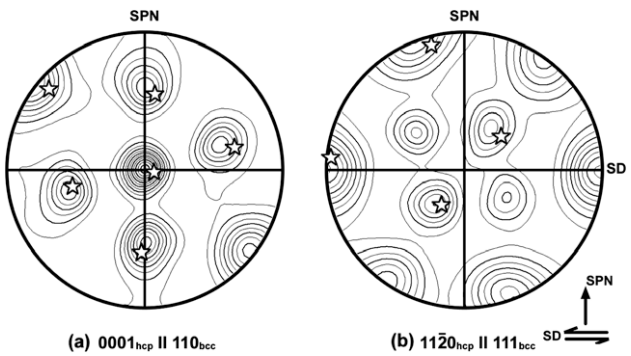

Figure 4. $\{110\}_{bcc}$ and $\{111\}_{bcc}$ pole figures displaying the positions of the peaks observed in the weld nugget of a β-titanium friction stir weld (starred) [16] superimposed on the α textures observed in the present study ($\{0001\}_{hcp}$ and $\{11\bar{2}0\}_{hcp}$ pole figures of the deposited weld from Figure 2(b)).

Beausir et al. [30] have recently studied the ideal crystallographic textures that develop during simple shear deformation of hcp crystals. One of these hcp shear texture components, the P_1 component, matches very well with both the central (and strongest) component in the $\{0001\}_{hcp}$ pole figure and the texture components around the peripheries of the $\{10\bar{1}0\}_{hcp}$ and $\{11\bar{2}0\}_{hcp}$ pole figures, all of which are also contained in the bcc $D_2(\bar{1}\bar{1}2)[111]$ shear texture. The elevated strength of these specific texture components suggests that this hcp P_1 shear component may also contribute to the observed texture, although the multiplicity of orientations in the $\{0001\}_{hcp}$ pole figure confirms the prevalence of the bcc $D_2(\bar{1}\bar{1}2)[111]$ shear texture.

In conclusion, friction stir welds in the near-α-titanium alloy, Ti-5111, have been examined by electron backscatter diffraction. The high temperatures and extensive shear deformation adjacent to the tool generate a microstructure of fine α laths within equiaxed prior-β grains. The resultant texture closely matches that of a $D_2(\bar{1}\bar{1}2)[111]$ bcc simple shear texture that was transformed to hcp according to the Burgers orientation relationship, aligning the $\{110\}_{bcc}$ and $\{0001\}_{hcp}$ planes parallel to each other. This indicates that the material is deformed above the β transus during welding and that the α texture is inherited directly from a simple shear texture of the high-temperature β phase. While this texture differs from that reported in friction stir welds in Ti-6Al-4V, it is similar to those produced during friction stir welding of a β-titanium alloy, friction stir processing of pure iron, and equal channel angular extrusion of bcc iron. However, the strength of some of the observed $D_2(\bar{1}\bar{1}2)[111]$ texture components indicate that an hcp P_1 shear texture component may also contribute to the observed texture.

This research is supported by the Office of Naval Research. The authors would also like to acknowledge Mr. K. Klug (Concurrent Technologies Corporation) and Mr. E. Czyryca (Naval Surface Warfare Center, Carderock Division) for supplying the plate used in this study and Prof. A. Rollett (Carnegie Mellon University) for helpful discussions. In addition, we thank Mr. L. Levenberry for his assistance with preparing the samples and Dr. D. Rowenhorst for his assistance with the EBSD.

[1] W.M. Thomas, E.D. Nicholas, J.C. Needham, M.G. Murch, P. Temple-Smith, C.J. Dawes, G.B. Patent Application No. 9,125,978.8, December 1991: U.S. Patent No. 5,460,317, 1995.
[2] K.V. Jata, S.L. Semiatin, Scripta Mater. 43 (2000) 743.
[3] D.P. Field, T.W. Nelson, Y. Hovanski, K.V. Jata, Metall. Mater. Trans. A 32 (2001) 2869.
[4] Y.S. Sato, H. Kokawa, K. Ikeda, M. Enomoto, S. Jogan, T. Hashimoto, Metall. Mater. Trans. A 32 (2001) 941.
[5] J.Q. Su, T.W. Nelson, R. Mishra, M. Mahoney, Acta Mater. 51 (2003) 713.
[6] R.W. Fonda, J.F. Bingert, K.J. Colligan, Scripta Mater. 51 (2004) 243.
[7] R.W. Fonda, J.F. Bingert, Metall. Mater. Trans. A 35A (2004) 1487.
[8] J.A. Schneider, A.C. Nunes, Metall. Mater. Trans. B 35 (2004) 777.
[9] J.Q. Su, T.W. Nelson, C.J. Sterling, Mater. Sci. Eng. A 405 (2005) 277.
[10] P.B. Prangnell, C.P. Heason, Acta Mater. 53 (2005) 3179.
[11] R.W. Fonda, J.F. Bingert, Metall. Mater. Trans. A 37A (2006) 3593.
[12] R.W. Fonda, J.F. Bingert, Scripta Mater. 57 (2007) 1052.
[13] Y.S. Sato, T.W. Nelson, C.J. Sterling, Acta Mater. 53 (2005) 637.
[14] Y.S. Sato, T.W. Nelson, C.J. Sterling, R.J. Steel, C.O. Pettersson, Mater. Sci. Eng. A 397 (2005) 376.
[15] A.J. Ramirez, M.C. Juhas, Mater. Sci. Forum 426–432 (2003) 2999.
[16] A.P. Reynolds, E. Hood, W. Tang, Scripta Mater. 52 (2005) 491.
[17] W.B. Lee, C.Y. Lee, W.S. Chang, Y.M. Yeon, S.B. Jung, Mater. Lett. 59 (2005) 3315.
[18] J. Been, K. Faller, JOM 51 (1999) 21.
[19] W.G. Burgers, Physica 1 (1934) 561.
[20] G. Lutjering, J.C. Williams, Titanium, Springer, New York, NY, 2003.
[21] R.W. Fonda, K.E. Knipling, J.F. Bingert, Scripta Mater. 58 (2008) 343.
[22] F. Montheillet, M. Cohen, J.J. Jonas, Acta Metall. 32 (1984) 2077.
[23] F. Montheillet, P. Gilormini, J.J. Jonas, Acta Metall. 33 (1985) 705.
[24] J. Baczynski, J. Jonas, Acta Mater. 44 (1996) 4273.
[25] A.D. Rollett, S.I. Wright, in: U.F. Kocks, S.N. Tome, H.R. Wenk (Eds.), Texture and Anisotropy, Cambridge University Press, 1998, p. 202.
[26] S. Mironov, Y. Zhang, Y.S. Sato, H. Kokawa, Scripta Mater. 59 (2008) 27.
[27] S. Mironov, Y.S. Sato, H. Kokawa, Acta Mater. 56 (2008) 2602.
[28] S. Li, I.J. Beyerlein, M.A.M. Bourke, Mater. Sci. Eng. A 394 (2005) 66.
[29] A.A. Gazder, F.D. Torre, C. Gu, C. Davies, E. Pereloma, Mater. Sci. Eng. A 415 (2006) 126.
[30] B. Beausir, L.S. Toth, K.W. Neale, Acta Mater. 55 (2007).